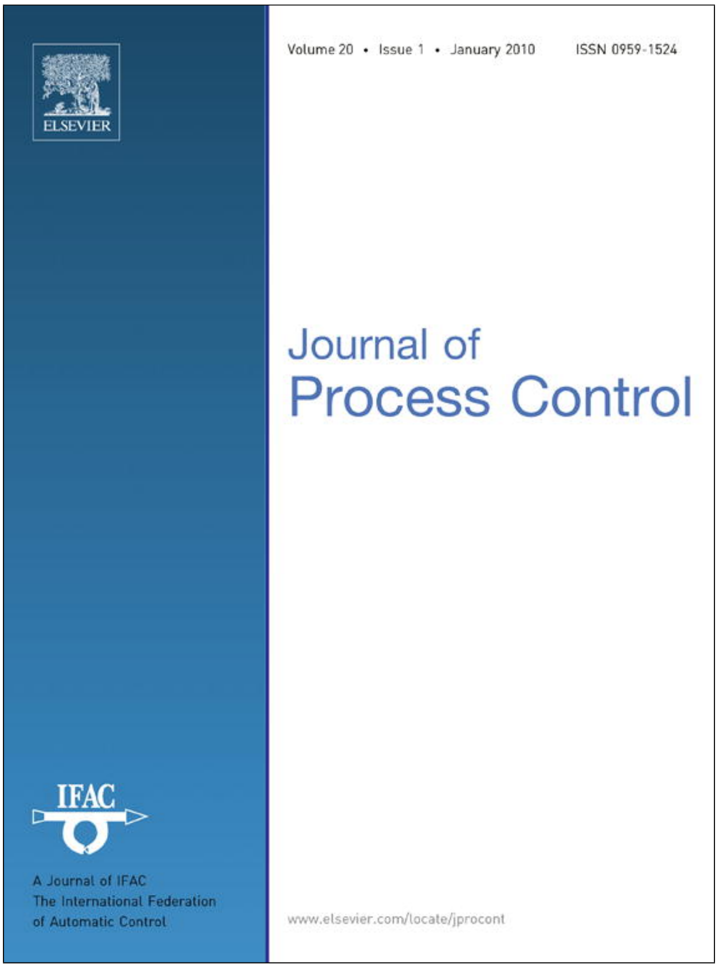
Volume 20 • Issue 1 • January 2010
ISSN 0959-1524
ELSEVIER
Journal of
Process Control
IFAC
A Journal of IFAC
The International Federation
of Automatic Control
www.elsevier.com/locate/jprocont

Journal of Process Control 20 (2010) 45–57

Contents lists available at ScienceDirect

Journal of Process Control

journal homepage: www.elsevier.com/locate/jprocont

On unscented Kalman filtering with state interval constraints

Bruno O.S. Teixeira [a,*], Leonardo A.B. Tôrres [a], Luis A. Aguirre [a], Dennis S. Bernstein [b]

[a] Department of Electronic Engineering, Federal University of Minas Gerais, Belo Horizonte, MG, Brazil
[b] Department of Aerospace Engineering, University of Michigan, Ann Arbor, MI, USA

ARTICLE INFO

Article history:
Received 20 November 2008
Received in revised form 15 October 2009
Accepted 15 October 2009

Keywords:
State estimation
Interval constraints
Unscented Kalman filter

ABSTRACT

This paper addresses the state-estimation problem for nonlinear systems for the case in which prior knowledge is available in the form of interval constraints on the states. Approximate solutions to this problem are reviewed and compared with new algorithms. All the algorithms investigated are based on the unscented Kalman filter. Two illustrative examples of chemical processes are discussed. Numerical results suggest that the use of constrained unscented filtering algorithms improves the accuracy of the state estimates compared to the unconstrained unscented filter, especially when a poor initialization is set. Moreover, it is shown that the constrained filters that enforce the state interval constraint on both the state estimate and error covariance yield more accurate state estimates than the methods that enforce such constraint only on the state estimates.

1. Introduction

The classical Kalman filter (KF) provides optimal state estimates under Gaussian disturbances and linear model assumptions [7]. In practice, however, the dynamics and disturbances may be such that the state vector is known to satisfy an inequality [5,21] or an equality [31] constraint. For example, in a chemical reaction, the species concentrations are nonnegative [3,6,15,20,35]. Additional examples of systems with inequality-constrained states arise in aeronautics [22,28]. The equality-constrained case is addressed in [30,31] and references therein and is outside the scope of this paper. However, Gaussian noise and an inequality-constrained state vector are mutually exclusive assumptions even for linear systems [5,18,19]. Therefore, for such systems, KF does not guarantee that its estimates satisfy the inequality constraint. In such cases, as well as for nonlinear systems, we wish to obtain state estimates that satisfy inequality constraints. In this paper, we are specifically concerned with interval constraints.

Constrained state estimation has received increasing attention in both academia and industry especially in the last 10 years [26]. Various approximate algorithms have been developed for inequality-constrained linear state estimation. One of the most popular techniques is the moving horizon estimator (MHE) [18], which formulates the state-estimation problem as a nonrecursive constrained quadratic program. Alternatively, probabilistic methods [22] enforce the inequality constraint by properly initializing the KF algorithm and tuning its noise covariances. The truncation procedure [24,25] reshapes the probability density function computed by KF, which is assumed to be Gaussian and is given by the state estimate and the error covariance, at the inequality constraint edges. Finally, if the state estimates do not satisfy the inequality constraint, then they are projected onto the boundary of the constraint region by the projection approach [25,28].

For nonlinear systems, algorithms based on MHE are employed [6,19,20,23]. However, since these techniques are nonrecursive, they are computationally expensive and difficult to use in some real-time applications [20,35,39]. For such cases, the constrained extended Kalman filter (CEKF) [19,35], which is a special case of MHE with unitary moving horizon and is called recursive nonlinear dynamics data reconciliation (RNDDR) in [35,36], is presented as a simpler and less computationally demanding algorithm. Motivated by the improved performance [10,11,14,32,37] of the unscented Kalman filter (UKF) [9,10] over the extended Kalman filter (EKF) [7], the unscented RNDDR, which is referred to as the sigma-point interval unscented Kalman filter (SIUKF) in this paper, is presented in [35]. Finally, constrained algorithms based on particle filtering [1] and the ensemble Kalman filer (EnKF) [4] are, respectively, presented in [13,17].

The present paper addresses the state-estimation problem for interval-constrained nonlinear systems. We review UKF and SIUKF and present approximate solutions to this problem based on UKF as follows. We combine either the unscented transform (UT) [9] or the interval-constrained UT (ICUT) [35], which are used during the forecast step of UKF and SIUKF, respectively, together with one of the following data-assimilation approaches, namely, (i) the classical KF update [7,9], (ii) the constrained Kalman update

* Corresponding author.
E-mail addresses: brunoot@cpdee.ufmg.br (B.O.S. Teixeira), torres@cpdee.ufmg.br (L.A.B. Tôrres), aguirre@cpdee.ufmg.br (L.A. Aguirre), dsbaero@umich.edu (D.S. Bernstein).

0959-1524/$ - see front matter
doi:10.1016/j.jprocont.2009.10.007

of CEKF [29,34,35], (iii) the sigma-point constrained update of SIUKF [12,16,17,35], (iv) the classical KF update followed by either the estimate projection approach [28], or (v) the truncation procedure [24,25]. Then we obtain eight new algorithms, namely, the constrained UKF (CUKF), the constrained interval UKF (CIUKF), the interval UKF (IUKF), the sigma-point UKF (SUKF), the projected UKF (PUKF), the projected interval UKF (PIUKF), the truncated UKF (TUKF), and the truncated interval UKF (TIUKF); see Table 1. These algorithms are compared to UKF and SIUKF in terms of accuracy and processing time by means of two illustrative examples that are commonly investigated in the literature, namely, a batch reactor [11,12,17,20,34,35] and a continuously stirred tank reactor [6,12,33]. In doing so, the interested reader may compare the performance of the unscented filtering approaches investigated in this paper with those presented in the literature, namely, EKF [6,11,12,34], CEKF [12,34], MHE [6,12], particle filter [20], and constrained EnKF [17]. Our goal is to obtain nonnegative state estimates. The challenge in these examples is that they have multi-modal probability density functions (PDFs).

The present paper is based on research in [29], while a preliminary version of it appears as [33].

2. State estimation for nonlinear systems

For the stochastic nonlinear discrete-time dynamic system

$$x_k = f(x_{k-1}, u_{k-1}, k-1) + w_{k-1}, \tag{2.1}$$

$$y_k = h(x_k, k) + v_k, \tag{2.2}$$

where $f : \mathbb{R}^n \times \mathbb{R}^p \times \mathbb{N} \to \mathbb{R}^n$ and $h : \mathbb{R}^n \times \mathbb{N} \to \mathbb{R}^m$ are, respectively, the process and observation models, the state-estimation problem can be described as follows. Assume that, for all $k \geqslant 1$, the known data are the measurements $y_k \in \mathbb{R}^m$, the inputs $u_{k-1} \in \mathbb{R}^p$, and the PDFs $\rho(x_0)$, $\rho(w_{k-1})$ and $\rho(v_k)$, where $x_0 \in \mathbb{R}^n$ is the initial state vector, $w_{k-1} \in \mathbb{R}^n$ is the process noise, and $v_k \in \mathbb{R}^m$ is the measurement noise. Next, define the profit function

$$J(x_k) \triangleq \rho(x_k|(y_1,\ldots,y_k)), \tag{2.3}$$

which is the value of the conditional PDF of the state vector $x_k \in \mathbb{R}^n$ given the past and present measured data $y_1,\ldots,y_k$. Under the stated assumptions, the maximization of (2.3) is the state-estimation problem, while the maximizer (mode) of J is the optimal state estimate [6,20].

The solution to this problem is complicated by the fact that, for nonlinear systems, $\rho(x_k|(y_1,\ldots,y_k))$ is not completely characterized by its mean $\hat{x}_{k|k}$ and covariance $P^{xx}_{k|k} \triangleq \mathscr{E}[(x_k - \hat{x}_{k|k})(x_k - \hat{x}_{k|k})^{\mathrm{T}}]$. We thus use an approximation based on the classical Kalman filter (KF) for linear systems [7] to provide a suboptimal solution to the nonlinear case, specifically, the unscented Kalman filter (UKF) [9]. To accomplish that, UKF propagates only approximations to $\hat{x}_{k|k}$ and $P^{xx}_{k|k}$ using the initial mean $\hat{x}_{0|0}$ and the covariance $P^{xx}_{0|0} \triangleq \mathscr{E}[(x_0 - \hat{x}_{0|0})(x_0 - \hat{x}_{0|0})^{\mathrm{T}}]$ of $\rho(x_0)$, which are assumed to be known. We assume that the approximation to the mean $\hat{x}_{k|k}$ provided by UKF is close to the maximizer of J. Furthermore, we assume that the mean and covariance of $\rho(w_{k-1})$ and $\rho(v_k)$ are known and equal to zero and Q_{k-1}, R_k, respectively. Also, w_{k-1} and v_k are assumed to be uncorrelated.

Table 1
Interval-constrained state estimators based on the unconstrained UKF. We make explicit the procedure used during the forecast step (column-wise), as well as the type of KF update used during data-assimilation (row-wise). Inside parentheses, we cite the section in which the method is either reviewed (*) or presented.

Data assimilation\forecast	UT (3.1) [9]	ICUT (5.1.1) [11,35]
Classical KF update (3.2) [7,9]	UKF* (3.2)	IUKF (6.4)
Constrained KF update (5.2.1) [29,34,35]	CUKF (6.2)	CIUKF (6.3)
Sigma-point constrained update (5.2.2) [12,16,17,35]	SUKF (6.5)	SIUKF* (6.1)
Classical KF update plus projection (5.2.3) [28]	PUKF (6.6)	PIUKF (6.7)
Classical KF update plus truncation (5.2.4) [24,25]	TUKF (6.8)	TIUKF (6.9)

3. Unscented Kalman filter

3.1. The unscented transform

Instead of analytically or numerically linearizing (2.1) and (2.2) and using the KF equations [7], UKF employs the *unscented transform* (UT) [9], which approximates the mean $\hat{y}_k \in \mathbb{R}^m$ and covariance $P^{yy}_k \in \mathbb{R}^{m\times m}$ of the random vector y_k obtained from the nonlinear transformation $y_k = h(x_k)$, where x_k is a random vector whose mean $\hat{x}_k \in \mathbb{R}^n$ and covariance $P^{xx}_k \in \mathbb{R}^{n\times n}$ are assumed to be known.

UT is based on a set of deterministically chosen vectors $\mathscr{X}_{j,k} \in \mathbb{R}^n, j = 0,\ldots,2n$, known as sigma points. To satisfy

$$\sum_{j=0}^{2n} \gamma_j \mathscr{X}_{j,k} = \hat{x}_k \quad \text{and} \quad \sum_{j=0}^{2n} \gamma_j [\mathscr{X}_{j,k} - \hat{x}_k][\mathscr{X}_{j,k} - \hat{x}_k]^{\mathrm{T}} = P^{xx}_k \tag{3.1}$$

with weights $\gamma \triangleq [\gamma_0 \gamma_1 \ldots \gamma_{2n}] \in \mathbb{R}^{2n+1}$ satisfying $\sum_{j=0}^{2n}\gamma_j = 1$ given by

$$\gamma_0 \triangleq \frac{\lambda}{n+\lambda}, \quad \gamma_j \triangleq \frac{1}{2(n+\lambda)}, \quad j = 1,\ldots,2n, \tag{3.2}$$

the sigma-point matrix $\mathscr{X}_k \triangleq [\mathscr{X}_{0,k} \mathscr{X}_{1,k} \ldots \mathscr{X}_{2n,k}] \in \mathbb{R}^{n\times(2n+1)}$ is chosen as

$$\mathscr{X}_k = \hat{x}_k 1_{1\times(2n+1)} + \sqrt{n+\lambda}\left[0_{n\times 1} \ (P^{xx}_k)^{1/2} \ -(P^{xx}_k)^{1/2}\right], \tag{3.3}$$

where $(\cdot)^{1/2}$ is the Cholesky square root and $\lambda > -n$. For notational simplicity, we refer to (3.2) and (3.3) as the function Ψ_{UT}, which is defined by

$$[\gamma, \mathscr{X}_k] \triangleq \Psi_{\mathrm{UT}}(\hat{x}_k, P^{xx}_k, n, \lambda). \tag{3.4}$$

Propagating each sigma point through h yields

$$\mathscr{Y}_{j,k} = h(\mathscr{X}_{j,k}), \quad j = 0,\ldots,2n,$$

such that

$$\hat{y}_k = \sum_{j=0}^{2n} \gamma_j \mathscr{Y}_{j,k} \quad \text{and} \quad P^{yy}_k = \sum_{j=0}^{2n} \gamma_j [\mathscr{Y}_{j,k} - \hat{y}_k][\mathscr{Y}_{j,k} - \hat{y}_k]^{\mathrm{T}}.$$

Alternative schemes for choosing sigma points are given in [9].

Henceforth, the notation $\hat{x}_{k|k-1}$ indicates an estimate of x_k at time k based on information available up to and including time $k-1$. Likewise, $\hat{x}_{k|k}$ indicates an estimate of x_k at time k using information available up to and including time k. Furthermore, $\hat{x}_{j,k|k}$ is the jth entry of $\hat{x}_{k|k}$, while $P^{xx}_{(i,j),k|k}$ is the (i,j) entry of $P^{xx}_{k|k}$.

3.2. The UKF algorithm

UKF is a two-step estimator whose *forecast* step is given by

$$[\gamma, \mathscr{X}_{k-1|k-1}] = \Psi_{\mathrm{UT}}(\hat{x}_{k-1|k-1}, P^{xx}_{k-1|k-1}, n, \lambda), \tag{3.5}$$

$$\mathscr{X}_{j,k|k-1} = f(\mathscr{X}_{j,k-1|k-1}, u_{k-1}, k-1), \quad j = 0,\ldots,2n, \tag{3.6}$$

$$\hat{x}_{k|k-1} = \sum_{j=0}^{2n} \gamma_j \mathscr{X}_{j,k|k-1}, \tag{3.7}$$

$$P^{xx}_{k|k-1} = \sum_{j=0}^{2n} \gamma_j [\mathscr{X}_{j,k|k-1} - \hat{x}_{k|k-1}][\mathscr{X}_{j,k|k-1} - \hat{x}_{k|k-1}]^{\mathrm{T}} + Q_{k-1}, \tag{3.8}$$

$$[\gamma, \mathscr{X}_{k|k-1}] = \Psi_{\mathrm{UT}}(\hat{x}_{k|k-1}, P^{xx}_{k|k-1}, n, \lambda), \tag{3.9}$$

$$\mathscr{Y}_{j,k|k-1} = h(\mathscr{X}_{j,k|k-1}, k), \quad j = 0,\ldots,2n, \tag{3.10}$$

$$\hat{y}_{k|k-1} = \sum_{j=0}^{2n} \gamma_j \mathscr{Y}_{j,k|k-1}, \tag{3.11}$$

$$P^{yy}_{k|k-1} = \sum_{j=0}^{2n} \gamma_j [\mathscr{Y}_{j,k|k-1} - \hat{y}_{k|k-1}][\mathscr{Y}_{j,k|k-1} - \hat{y}_{k|k-1}]^{\mathrm{T}} + R_k, \tag{3.12}$$

$$P^{xy}_{k|k-1} = \sum_{j=0}^{2n} \gamma_i [\mathscr{X}_{j,k|k-1} - \hat{x}_{k|k-1}][\mathscr{Y}_{j,k|k-1} - \hat{y}_{k|k-1}]^{\mathrm{T}}, \tag{3.13}$$

where $P^{xx}_{k|k-1}$ is the forecast error covariance, $P^{yy}_{k|k-1}$ is the innovation covariance, $P^{xy}_{k|k-1}$ is the cross covariance, and $P^{xx}_{k|k}$ is the data-assimilation error-covariance, and whose *data-assimilation* step is given by the *classical KF update*, that is,

$$K_k = P^{xy}_{k|k-1}(P^{yy}_{k|k-1})^{-1}, \tag{3.14}$$

$$\hat{x}_{k|k} = \hat{x}_{k|k-1} + K_k(y_k - \hat{y}_{k|k-1}), \tag{3.15}$$

$$P^{xx}_{k|k} = P^{xx}_{k|k-1} - K_k P^{yy}_{k|k-1} K_k^{\mathrm{T}}, \tag{3.16}$$

where $K_k \in \mathbb{R}^{n\times m}$ is the Kalman gain matrix. Model information is used during the forecast step, while measurement data are injected into the estimates during the data-assimilation step.

4. State estimation for interval-constrained nonlinear systems

Assume that, for all $k \geqslant 0$, the state vector x_k satisfies the interval constraint

$$d_k \leqslant x_k \leqslant e_k, \tag{4.1}$$

where $d_k \in \mathbb{R}^n$ and $e_k \in \mathbb{R}^n$ are assumed to be known and, for $j = 1, \dots, n, d_{j,k} < e_{j,k}$. Also, if $x_{j,k}$ is left-unbounded or right-unbounded, then we set $d_{j,k} = -\infty$ or $e_{j,k} = \infty$, respectively. Thus, the objective of the interval-constrained state-estimation problem is to maximize (2.3) subject to (4.1).

In addition to nonlinear dynamics, the solution to this problem is complicated due the inclusion of interval constraints. We thus extend approximate algorithms derived in the linear scenario to provide suboptimal estimates in the nonlinear case.

5. Approaches to enforce interval constraints: Review

We now discuss the main approaches used in the literature to enforce state interval constraints in each step of the state estimator, namely, the forecast and data assimilation steps, as indicated in Table 1.

5.1. Forecast step

5.1.1. The interval-constrained unscented transform

Recall that UT given by (3.4) does not enforce the interval constraint into the sigma points. On the other hand, the *interval-constrained unscented transform* (ICUT) [35] generates sigma points satisfying

$$d_k \leqslant \mathscr{X}_{j,k} \leqslant e_k, \quad j = 0, \dots, 2n. \tag{5.1}$$

To do so, unlike in (3.3), $\mathscr{X}_k$ is chosen as

$$\begin{aligned}\mathscr{X}_k = \hat{x}_k 1_{1\times(2n+1)} + \Big[0_{n\times 1}\ \theta_{1,k}\mathrm{col}_1\left[(P_k^{xx})^{1/2}\right] \dots \theta_{n,k}\mathrm{col}_n\left[(P_k^{xx})^{1/2}\right] \\ -\theta_{n+1,k}\ \mathrm{col}_{n+1}\left[(P_k^{xx})^{1/2}\right] \dots - \theta_{2n,k}\mathrm{col}_{2n}[(P_k^{xx})^{1/2}]\Big],\end{aligned} \tag{5.2}$$

where, for $i = 1, \dots, n$ and $j = 1, \dots, 2n$,

$$\theta_{j,k} \triangleq \min(\mathrm{col}_j(\Theta)), \tag{5.3}$$

$$\Theta_{(i,j)} \triangleq \begin{cases} \sqrt{n+\lambda}, & \text{if } S_{(i,j)} = 0, \\ \min\left(\sqrt{n+\lambda}, \frac{e_{i,k} - \hat{x}_{i,k}}{S_{(i,j)}}\right), & \text{if } S_{(i,j)} > 0, \\ \min\left(\sqrt{n+\lambda}, \frac{d_{i,k} - \hat{x}_{i,k}}{S_{(i,j)}}\right), & \text{if } S_{(i,j)} < 0, \end{cases} \tag{5.4}$$

$$S \triangleq \left[(P_k^{xx})^{1/2} \quad -(P_k^{xx})^{1/2}\right] \tag{5.5}$$

with time-varying weights $\gamma_k \triangleq [\gamma_{0,k}\gamma_{1,k} \cdots \gamma_{2n,k}] \in \mathbb{R}^{2n+1}$ satisfying $\sum_{j=0}^{2n} \gamma_{j,k} = 1$ given by

$$\gamma_{0,k} \triangleq b_k, \quad \gamma_{j,k} \triangleq a_k\theta_{j,k} + b_k, \quad j = 1, \dots, 2n \tag{5.6}$$

where

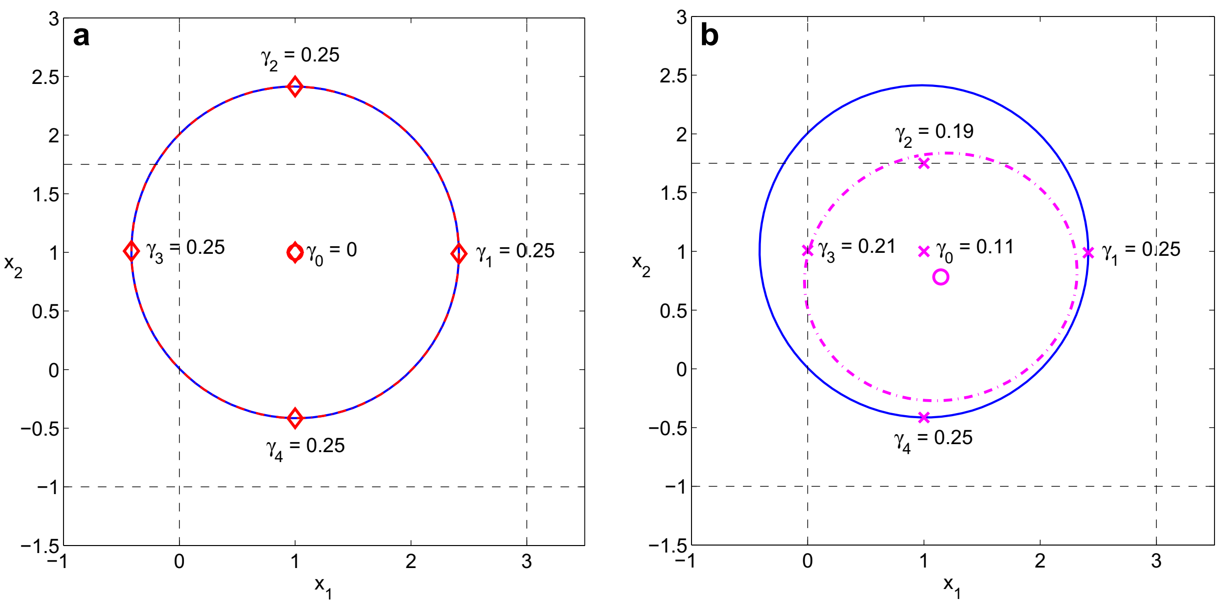

Fig. 1. Sigma points of (a) UT ($\diamond$) in comparison with those of (b) ICUT ($\times$) and related weights for an example where $x_k \in \mathbb{R}^2, \hat{x}_k = [11]^{\mathrm{T}}, P_k^{xx} = I_{2\times2}, d_k = [0 \quad -1]^{\mathrm{T}}, e_k = [3 \quad 1.75]^{\mathrm{T}}$, and $\lambda = 0$. The circle ($\circ$) represents the weighted mean of sigma points, the dot-dashed ($-\cdot-$) line denotes the corresponding covariance, and the solid (– – –) line is the true covariance. For UT, these lines coincide.

$$a_k \triangleq \frac{2\lambda - 1}{2(n+\lambda)\left(\sum_{j=1}^{n}\theta_{j,k} - (2n+1)\sqrt{n+\lambda}\right)}, \tag{5.7}$$

$$b_k \triangleq \frac{1}{2(n+\lambda)} - \frac{2\lambda - 1}{(2\sqrt{n+\lambda})\left(\sum_{j=1}^{n}\theta_{j,k} - (2n+1)\sqrt{n+\lambda}\right)}. \tag{5.8}$$

For notational simplicity, we refer to (5.2)–(5.8) as the function $\Psi_{\rm ICUT}$, which is defined by

$$[\gamma_k, \mathscr{X}_k] \triangleq \Psi_{\rm ICUT}(\hat{x}_k, P_k^{xx}, d_k, e_k, n, \lambda). \tag{5.9}$$

From (5.2), note that ICUT assumes that $\hat{x}_k$ satisfies (4.1); otherwise, $\mathscr{X}_{0,k}$ does not satisfy (5.1). Therefore, if, during the filter implementation, $\hat{x}_k$ does not satisfy (4.1), then $\hat{x}_k$ must be projected onto the boundary of (4.1) before using (5.9).

Also, note that, for UT, $\theta_{j,k} = \sqrt{n+\lambda}$, for all $k \geqslant 1$ and $j = 0, \ldots, 2n$; see (3.3). Fig. 1 illustrates how the sigma points of ICUT are chosen compared to UT. Note that whenever a sigma point violates (5.1), the sigma point is projected onto the boundary of the constraint region defined by (4.1) and the corresponding weight is changed. That is, the sigma points are *clipped* to satisfy (5.1). In doing so, unlike UT, the sigma points are not necessarily symmetric around $\hat{x}_k$ such that their weighted sample mean and covariance may not satisfy (3.1). However, unlike UT, both the weighted sample mean and covariance of such sigma points capture the interval constraint information.

ICUT is used in the forecast step of the sigma-point interval unscented Kalman filter (SIUKF) [35]. An approach similar to (5.2)–(5.8) is employed in [17] in the context of the ensemble Kalman filter (EnKF). The idea behind ICUT is also used in [11] to enforce linear inequality constraints and in [8] to enforce nonlinear equality constraints into the UKF estimates.

5.2. Data-assimilation step

5.2.1. Constrained KF update

Recall that, assuming that x_0, w_{k-1}, and v_k are Gaussian and that f and h are linear, $\hat{x}_{k|k}$ given by (3.15) is the maximizer of (2.3), or, equivalently, the minimizer of [7, pp. 207–208]

$$J_1(x_k) \triangleq \Big[(y_k - h(x_k,k))^{\rm T} R_k^{-1}(y_k - h(x_k,k)) + (x_k - \hat{x}_{k|k-1})^{\rm T}(P_{k|k-1}^{xx})^{-1}(x_k - \hat{x}_{k|k-1})\Big]. \tag{5.10}$$

That is, KF yields

$$\hat{x}_{k|k} = \arg x_k \min J_1(x_k).$$

Thus, EKF and UKF employ the classical KF update given by (3.14)–(3.16) to suboptimally assimilate the measured data into the estimates, but without enforcing any state constraints into them.

Motivated by the result above, to enforce state constraints, the constrained extended Kalman filter (CEKF) [19,35] replaces (3.15) of the classical KF update by the constrained optimization problem

$$\hat{x}_{k|k} = \mathop{\arg\min}_{\{x_k : d_k \leqslant x_k \leqslant e_k\}} J_1(x_k), \tag{5.11}$$

yielding the *constrained KF update* given by (3.14), (5.11), and (3.16). However, by using (3.16) to update the pseudo-error covariance $P_{k|k}^{xx}$, the constraint information is not enforced into it.

Also, note that nonlinear inequality and equality constraints may be enforced into $\hat{x}_{k|k}$ using the optimization approach given by (5.11).

5.2.2. Sigma-point constrained KF update

In the unconstrained scenario, it is shown that the data-assimilation equations of UKF given by (3.15) and (3.16) are equivalent to [12, Appendix A]

$$\mathscr{X}_{j,k|k} = \mathscr{X}_{j,k|k-1} + K_k(y_k - \mathscr{Y}_{j,k|k-1}), \tag{5.12}$$

$$\hat{x}_{k|k} = \sum_{j=0}^{2n} \gamma_j \mathscr{X}_{j,k|k}, \tag{5.13}$$

$$P_{k|k}^{xx} = \sum_{j=0}^{2n} \gamma_j [\mathscr{X}_{j,k|k} - \hat{x}_{k|k}][\mathscr{X}_{j,k|k} - \hat{x}_{k|k}]^{\rm T}, \tag{5.14}$$

where $\mathscr{X}_{j,k|k-1}, \mathscr{Y}_{j,k|k-1}$, and K_k are given by (3.9), (3.10) and (3.14), respectively. Also, note that the data assimilation step of EnKF is implemented as (5.12)–(5.14) [4].

Then, combining the sigma-point KF update of UKF given by (5.12)–(5.14) with the constrained KF update given by (3.14), (5.11), and (3.16) yields the *sigma-point constrained KF update* given by

$$\mathscr{X}_{j,k|k} = \mathop{\arg\min}_{\{\mathscr{X}_{j,k} : d_k \leqslant \mathscr{X}_{j,k} \leqslant e_k\}} J_2(\mathscr{X}_{j,k}), \quad j = 0, \ldots, 2n, \tag{5.15}$$

together with (5.13) and (5.14), where

$$J_2(\mathscr{X}_{j,k}) \triangleq \Big[(y_k - h(\mathscr{X}_{j,k},k))^{\rm T} R_k^{-1}(y_k - h(\mathscr{X}_{j,k},k)) + (\mathscr{X}_{j,k} - \mathscr{X}_{j,k|k-1})^{\rm T}(P_{k|k-1}^{xx})^{-1}(\mathscr{X}_{j,k} - \mathscr{X}_{j,k|k-1})\Big] \tag{5.16}$$

and each column of $\mathscr{X}_{k|k} \triangleq [\mathscr{X}_{0,k|k}\mathscr{X}_{1,k|k} \ldots \mathscr{X}_{2n,k|k}] \in \mathbb{R}^{n\times(2n+1)}$ is the solution of the jth nonlinear constrained optimization problem (5.15).

Note that (5.13)–(5.15) enforces the constraint information into both state estimate and error covariance. Also, note that nonlinear inequality and equality constraints can be enforced into $\mathscr{X}_{j,k|k}$ using (5.15).

The sigma-point constrained KF update comprises the data-assimilation step of SIUKF [35]. In [16], to improve the accuracy of the propagation of $P_{k|k}^{xx}$ in (5.14), a modified version of (5.13)–(5.15) is presented.

5.2.3. Estimate projection

In the *estimate projection* approach, if the data-assimilation state estimate $\hat{x}_{k|k}$ given by (3.15) does not satisfy the interval constraint (4.1), then it is projected onto the boundary of the constraint region by solving the quadratic programming problem [25,28]

$$\hat{x}_{k|k}^{\rm p} = \mathop{\arg\min}_{\{x_k : d_k \leqslant x_k \leqslant e_k\}} J_3(x_k), \tag{5.17}$$

where

$$J_3(x_k) \triangleq (x_k - \hat{x}_{k|k})^{\rm T} W_k^{-1}(x_k - \hat{x}_{k|k}),$$

and $W_k \in \mathbb{R}^{n\times n}$ is a positive-definite weighting matrix. Similar to [28], we set $W_k = P_{k|k}^{xx}$, where $P_{k|k}^{xx}$ is given by (3.16).

The projection approach is used to enforce linear inequality constraints in the context of EKF in [28]. Also, it is employed to enforce nonlinear equality constraints in the context of EKF [27] and UKF [31].

5.2.4. PDF truncation

The *PDF truncation* procedure [24,25] is outlined as follows. Let $\hat{x}_{k|k}$ given by (3.15) and $P_{k|k}^{xx}$ given by (3.16) be, respectively, the pseudo-mean and pseudo-covariance of $\rho(x_k|(y_1, \ldots, y_k))$ obtained from UKF (Section 3) or from another KF extension. We want to truncate $\rho(x_k|(y_1, \ldots, y_k))$ at the n constraint edges given by the rows of the state interval constraint (4.1) such that the pseudo-mean $\hat{x}_{k|k}^{\rm t}$ of the truncated PDF is an interval-constrained state estimate with truncated error covariance $P_{k|k}^{xxt}$. This procedure is called PDF truncation [24,25] and is reviewed in Appendix A.

For example, consider the case where, even though $\hat{x}_{k|k} = [1 \quad 1]^T$ satisfies the interval constraint (4.1) with parameters $d_k = [0 \quad -1]^T$ and $e_k = [3 \quad 1.75]^T, P^{xx}_{k|k} = I_{2\times 2}$ has significant area outside (4.1); as shown in the solid line of Fig. 2. Thus, $\hat{x}^t_{k|k} = [1.23 \quad 0.67]^T$ is obtained by shifting $\hat{x}_{k|k}$ towards the centroid of the truncated PDF and $P^{xxt}_{k|k} = \mathrm{diag}(0.52, 0.45)$ is obtained by truncating $P^{xx}_{k|k}$ due the prior knowledge provided by (4.1).

While, in the projection approach, the data-assimilation state estimate $\hat{x}_{k|k}$ is projected onto the boundary of the interval constraint if it does not satisfy the interval constraint, in the PDF truncation approach, the PDF computed by UKF can be reshaped at the interval constraint edges even if $\hat{x}_{k|k}$ satisfies the interval constraint, as shown in Fig. 2. For both approaches, a third step must be appended to the filter equations; see Fig. 3. Such step is called *truncation* step for the PDF truncation approach.

The PDF truncation procedure is used in [24] in the context of EKF to enforce linear inequality constraints. Also, the truncation approach can be readily extended to handle linear equality constraints [25].

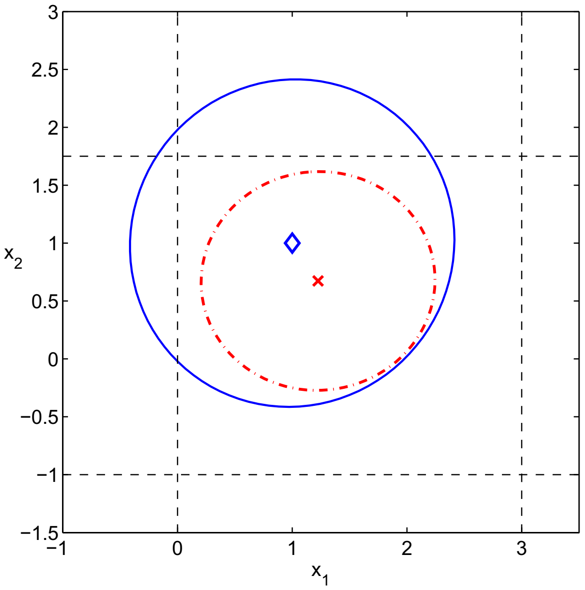

Fig. 2. The unconstrained estimate $\hat{x}_{k|k} = [1 \quad 1]^T$ ($\diamond$) satisfying the interval constraint (4.1) (– –) with $d_k = [0 - 1]^T$ and $e_k = [3 \quad 1.75]^T$ and its covariance $P^{xx}_{k|k} = I_{2\times 2}$ (– – –) with significant area outside (4.1) compared to the truncated estimate $\hat{x}^t_{k|k}$ ($\times$) and covariance $P^{xxt}_{k|k}$ (– · –).

6. Interval-constrained unscented Kalman filters

We now combine the approaches reviewed in Section 5 to enforce state interval constraints, yielding the algorithms listed in Table 1.

6.1. Sigma-point interval unscented Kalman filter

SIUKF combines ICUT during the forecast step with the sigma-point constrained KF update for data assimilation. Thus, SIUKF is a two-step estimator whose forecast step is given by [16,35]

$$[\gamma_{k-1}, \mathscr{X}_{k-1|k-1}] = \Psi_{\mathrm{ICUT}}(\hat{x}_{k-1|k-1}, P^{xx}_{k-1|k-1}, d_{k-1}, e_{k-1}, n, \lambda), \tag{6.1}$$

$$\mathscr{X}_{j,k|k-1} = f(\mathscr{X}_{j,k-1|k-1}, u_{k-1}, k-1), \quad j = 0, \ldots, 2n, \tag{6.2}$$

$$\hat{x}_{k|k-1} = \sum_{j=0}^{2n} \gamma_{j,k-1} \mathscr{X}_{j,k|k-1}, \tag{6.3}$$

$$P^{xx}_{k|k-1} = \sum_{j=0}^{2n} \gamma_{j,k-1} [\mathscr{X}_{j,k|k-1} - \hat{x}_{k|k-1}][\mathscr{X}_{j,k|k-1} - \hat{x}_{k|k-1}]^T + Q_{k-1}, \tag{6.4}$$

$$[\gamma_k, \mathscr{X}_{k|k-1}] = \Psi_{\mathrm{ICUT}}(\hat{x}_{k|k-1}, P^{xx}_{k|k-1}, d_k, e_k, n, \lambda), \tag{6.5}$$

and whose data-assimilation step is given by

$$\mathscr{X}_{j,k|k} = \underset{\{\mathscr{X}_{j,k} : d_k \leqslant \mathscr{X}_{j,k} \leqslant e_k\}}{\arg\min} J_2(\mathscr{X}_{j,k}), \quad j = 0, \ldots, 2n, \tag{6.6}$$

$$\hat{x}_{k|k} = \sum_{j=0}^{2n} \gamma_{j,k} \mathscr{X}_{j,k|k}, \tag{6.7}$$

$$P^{xx}_{k|k} = \sum_{j=0}^{2n} \gamma_{j,k} [\mathscr{X}_{j,k|k} - \hat{x}_{k|k}][\mathscr{X}_{j,k|k} - \hat{x}_{k|k}]^T, \tag{6.8}$$

where J_2 is given by (5.16). For clarity we repeat (3.6) as (6.2) and (5.15) as (6.6).

SIUKF enforces (5.1) during both the forecast (6.1), (6.5) and data-assimilation (6.6) steps. Therefore, not only $\hat{x}_{k|k-1}$ and $\hat{x}_{k|k}$, but also $P^{xx}_{k|k-1}$ and $P^{xx}_{k|k}$, assimilate the interval-constraint information.

6.2. Constrained unscented Kalman filter

We now present the constrained unscented Kalman filter (CUKF). Combining UT for forecast and the constrained KF update for data assimilation, CUKF is the straightforward unscented-based extension of CEKF. Recall that CEKF is a special case of the moving horizon estimator (MHE) with a unitary moving horizon [19]. Also, CUKF is addressed in the context of equality-constrained state estimation in [31].

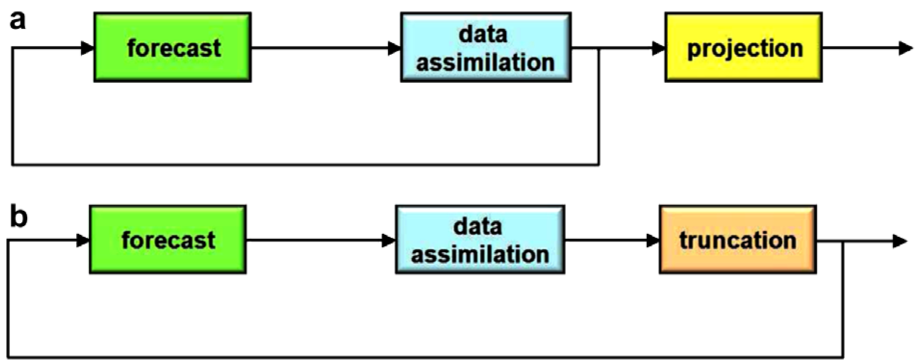

Fig. 3. Diagram of (a) PUKF and PIKF and (b) TUKF and TIUKF. Unlike the projection step of PUKF and PIUKF, the truncation step of TUKF and TIUKF is connected by feedback recursion.

Similar to UKF, CUKF is a two-step estimator. Its forecast step is given by (3.5)–(3.13). To enforce the state interval constraint (4.1), we replace (3.15) of UKF by the constrained optimization problem (5.11) such that the data-assimilation step of CUKF is given by (3.14), (5.11), and (3.16).

6.3. Constrained interval unscented Kalman filter

We now present the constrained interval unscented Kalman filter (CIUKF) as a simplified version of SIUKF. CIUKF is a two-step estimator whose forecast step is given by (6.1)–(6.5) together with

$$\mathcal{Y}_{j,k|k-1} = h(\mathcal{X}_{j,k|k-1}, k), \quad j = 0, \ldots, 2n, \tag{6.9}$$

$$\hat{y}_{k|k-1} = \sum_{j=0}^{2n} \gamma_{j,k} \mathcal{Y}_{j,k|k-1}, \tag{6.10}$$

$$P^{yy}_{k|k-1} = \sum_{j=0}^{2n} \gamma_{j,k} [\mathcal{Y}_{j,k|k-1} - \hat{y}_{k|k-1}][\mathcal{Y}_{j,k|k-1} - \hat{y}_{k|k-1}]^{\mathrm{T}} + R_k, \tag{6.11}$$

$$P^{xy}_{k|k-1} = \sum_{j=0}^{2n} \gamma_{j,k} [\mathcal{X}_{j,k|k-1} - \hat{x}_{k|k-1}][\mathcal{Y}_{j,k|k-1} - \hat{y}_{k|k-1}]^{\mathrm{T}} \tag{6.12}$$

and whose data-assimilation step is given by (3.14), (5.11), and (3.16). For clarity we repeat (3.10) as (6.9).

Note that the forecast steps of both CIUKF and SIUKF use ICUT, while the data-assimilation steps of CIUKF and CUKF are equal. That is, the data-assimilation step of CIUKF is a single sigma-point special case of the data-assimilation step of SIUKF. However, unlike SIUKF, $P^{xx}_{k|k}$ of CIUKF and CUKF are not affected by the state interval constraint (4.1).

6.4. Interval unscented Kalman filter

The interval unscented Kalman filter (IUKF), which is a simplified version of CIUKF, is a two-step estimator whose forecast step is given by (6.1)–(6.5), (6.9)–(6.12) and whose data-assimilation step is given by (3.14)–(3.16).

That is, the IUKF forecast equations are equal to the forecast equations of SIUKF and CIUKF, which uses ICUT, and its data-assimilation equations are equal to the data-assimilation equations of UKF. Unlike in SIUKF and CIUKF, the state interval constraint (4.1) is not enforced during data assimilation by IUKF. In [11] it is presented an algorithm similar to IUKF.

6.5. Sigma-point unscented Kalman filter

The sigma-point unscented Kalman filter (SUKF), which is a simplified version of SIUKF, is a two-step estimator whose forecast step is given by (3.5)–(3.9) and whose data-assimilation step is given by (6.6)–(6.8).

That is, the SUKF forecast equations are similar to the forecast equations of UKF and its data-assimilation equations are equal to the data-assimilation equations of SIUKF. That is, unlike in SIUKF and IUKF, the state interval constraint (4.1) is not enforced during forecast by SUKF. After submission of this paper, the authors came across with an article in press [12], wherein SUKF is presented as the nonlinear programming unscented Kalman filter (NLP-UKF).

6.6. Projected unscented Kalman filter

The projected unscented Kalman filter (PUKF) is the unscented-based nonlinear extension of the projected Kalman filter (PKF) [25,28], which considers inequality-constrained linear systems. PUKF is a three-step algorithm whose forecast step is given by (3.5)–(3.13), whose data-assimilation step is given by (3.14)–(3.16), and whose *projection* step is given by (5.17).

As shown in Fig. 3a, the constrained estimate $\hat{x}^{\mathrm{p}}_{k|k}$ is not recursively fed back in the forecast step at $k+1$; see (3.5) and [25,28] for further reference in the context of linear systems. It is intuitive to think that by feeding back the constrained state estimate in the forecast step we should obtain improved state estimates, as it is done in [31, Section 7.2] for equality-constrained systems. Note that this is somehow done by CUKF in (5.11), which can be seen as a PUKF algorithm that performs together the data-assimilation and projection steps.

6.7. Projected interval unscented Kalman filter

We now present the projected interval unscented Kalman filter (PIUKF) obtained from the combination of IUKF, which uses ICUT, and the projection approach of PUKF.

PIUKF is a three-step estimator whose forecast step is given by (6.1)–(6.5), (6.9)–(6.12), whose data-assimilation step is given by (3.14)–(3.16), and whose projection step is given by (5.17).

Note that PIUKF enforces the state interval constraint (4.1) during both the forecast step (on both $\hat{x}_{k|k-1}$ and $P^{xx}_{k|k-1}$) and projection step (only on $\hat{x}^{\mathrm{p}}_{k|k}$). Like in PUKF, the constrained estimate $\hat{x}^{\mathrm{p}}_{k|k}$ is not recursively fed back in the forecast step at $k+1$; see Fig. 3a.

6.8. Truncated unscented Kalman filter

We present the truncated unscented Kalman filter (TUKF) as the unscented-based nonlinear extension of the truncated Kalman filter (TKF) described in [25,29], which considers inequality-constrained linear systems, to the interval-constrained nonlinear state-estimation problem. Like TKF, the TUKF algorithm is obtained by appending the PDF truncation procedure to the UKF equations by feedback recursion; see Fig. 3b. That is, TUKF is a three-step algorithm whose forecast step is given by

$$[\gamma, \mathcal{X}_{k-1|k-1}] = \Psi_{\mathrm{UT}}(\hat{x}^{\mathrm{t}}_{k-1|k-1}, P^{xxt}_{k-1|k-1}, n, \lambda), \tag{6.13}$$

together with (3.6)–(3.13), whose data-assimilation step is given by (3.14)–(3.16), and whose *truncation* step is reviewed in Appendix A.

TUKF has two advantages. First, unlike SIUKF, SUKF, CIUKF, CUKF, PUKF, and PIUKF, it avoids the explicit online solution of a constrained optimization problem at each time step. Second, it assimilates the interval-constraint information in both the state estimate $\hat{x}^{\mathrm{t}}_{k|k}$ and the error covariance $P^{xxt}_{k|k}$.

6.9. Truncated interval unscented Kalman filter

We present now the truncated interval unscented Kalman filter (TIUKF) obtained from the combination of IUKF, which uses ICUT, and the PDF-truncation approach of TUKF. TIUKF is a three-step estimator whose forecast step is given by

$$[\gamma_{k-1}, \mathcal{X}_{k-1|k-1}] = \Psi_{\mathrm{ICUT}}(\hat{x}^{\mathrm{t}}_{k-1|k-1}, P^{xxt}_{k-1|k-1}, d_{k-1}, e_{k-1}, n, \lambda), \tag{6.14}$$

together with (6.2)–(6.5), (6.9)–(6.12), whose data-assimilation step is given by (3.14)–(3.16), and whose truncation step is equal to the truncation step of TUKF; see Appendix A and Fig. 3b.

Note that TIUKF enforces the state interval constraint (4.1) during both the forecast step (on both $\hat{x}_{k|k-1}$ and $P^{xx}_{k|k-1}$) and truncation step (on both $\hat{x}^{\mathrm{t}}_{k|k}$ and $P^{xxt}_{k|k}$).

6.10. Algorithms: summary of characteristics

In this section, we compare the structure of the UKF, SIUKF, CUKF, CIUKF, IUKF, SUKF, PUKF, PIUKF, TUKF, and TIUKF algorithms. Table 1 lists each algorithm with respect to the specific approaches used for the forecast and data-assimilation steps. Actually, TUKF, TIUKF, PUKF, and PIUKF are three-step algorithms that employ the classical KF update during the data-assimilation step and use a third step (truncation or projection) to enforce the interval constraint.

Moreover, Table 2 indicates, for each algorithm, whether or not the state estimates, as well as the pseudo-error covariance, are affected by the interval constraint in each step of the estimator. Also, we account for the number of constrained optimization problems that must be explicitly solved at each time step to enforce the state interval constraint (4.1).

Note that IUKF, TUKF, and TIUKF do not require the online solving of optimization problems to enforce interval constraints. As discussed in [17,35], such feature might be appealing for some real-time applications.

It is important to mention that some of the algorithms investigated in this paper can handle nonlinear inequality constraints and/or (linear and nonlinear) equality constraints in addition to the state interval constraint (4.1); see Table 2. Specifically, SIUKF, CUKF, CIUKF, and SUKF can handle nonlinear inequality and/or equality constraints during the data-assimilation step. Likewise, PUKF and PIUKF are able to enforce such constraints during the projection step, while TUKF and TIUKF can enforce linear equality constraints during the truncation step. If SIUKF, SUKF, TUKF, and TIUKF are used to enforce linear equality constraints, then the corresponding pseudo-error covariances ($P^{xx}_{k|k}$ or $P^{xxt}_{k|k}$) might become singular. In this case, in order to circumvent ill-conditioning problems in the forecast step at the next time step $k+1$, it is a common practice to sum up a small diagonal matrix (that is, a matrix whose entries are small enough compared to the original pseudo-error covariances) to $P^{xx}_{k|k}$ or $P^{xxt}_{k|k}$. For further details on equality-constrained Kalman filtering, see [31].

7. Numerical examples

7.1. Batch Reactor [11,12,17,20,34,35]

We consider the gas-phase reaction

$$2\mathrm{A} \xrightarrow{k_1} \mathrm{B},$$

with reaction-rate proportion $k_1 = 0.16$, taking place in a well-mixed, constant-volume, isothermal batch reactor. Let the state vector $x(t) \in \mathbb{R}^2_+$ be given by the partial pressures of A and B, whose dynamics are given by

$$\begin{bmatrix} \dot{x}_1(t) \\ \dot{x}_2(t) \end{bmatrix} = \begin{bmatrix} -2k_1 x_1^2(t) \\ k_1 x_1^2(t) \end{bmatrix}. \tag{7.1}$$

We set $x(0) = [\,3 \quad 1\,]^{\mathrm{T}}$.

To perform state estimation using UKF, SIUKF, CUKF, CIUKF, IUKF, SUKF, TUKF, TIUKF, PUKF, and PIUKF, we integrate the process model (7.1) with $T = 0.1$ s using the fourth-order Runge–Kutta algorithm such that $x_k \triangleq x(kT)$. We set $Q_{k-1} = 10^{-6} I_{2\times 2}$ to help convergence of estimates using UKF [38] with $\hat{x}_{0|0} = x_0$. For uniformity, this value is used in the remaining cases. We assume the reactor pressure is measured

$$y_k = [\,1 \quad 1\,] x_k + v_k, \tag{7.2}$$

where $R_k = 0.01$ is the variance of $v_k \in \mathbb{R}$. We want to enforce the interval constraint (4.1), where $d_k = 0_{2\times 1}$ and $e_k = \infty_{2\times 1}$. First, we set a poor initialization given by $\hat{x}_{0|0} = [0.1 \;\, 4.5]^{\mathrm{T}}$ and $P^{xx}_{0|0} = 36 I_{2\times 2}$ and we refer to it as case 1. Case 1 is also investigated in [35] using UKF and SIUKF; in [12] using EKF, UKF, SIUKF, and an algorithm similar to SUKF; in [17] using the constrained EnKF; in [20] using a particle filter, but resulting in biased estimates; and, finally, in [11] using EKF, UKF, and an algorithm similar to IUKF. We also investigate a second case (case 2) with good initialization given by $\hat{x}_{0|0} = [2.5 \;\, 0.5]^{\mathrm{T}}$ and $P^{xx}_{0|0} = 0.25 I_{2\times 2}$. Whenever a constrained optimization problem is solved, since the measurement model is linear, we use Matlab's function `quadprog`, which implements a subspace trust region optimization method for quadratic programming.

Fig. 4 presents a performance comparison among the aforementioned algorithms for a 100-run Monte Carlo simulation, regarding three performance indices: (i) root-mean-square error of the each state (RMSE_j)

$$\mathrm{RMSE}_j = \frac{1}{100} \sum_{m=1}^{100} \sqrt{\frac{1}{N} \sum_{k=}^{N} (x_{j,k} - \hat{x}_{j,k|k,m})^2}, \quad j = 1, \ldots, n, \tag{7.3}$$

where N is the final time and the subscript m refers to the mth Monte Carlo simulation; (ii) mean trace of the pseudo-error covariance matrix

$$\mathrm{MT} = \frac{1}{100N} \sum_{m=1}^{100} \sum_{k=1}^{N} \mathrm{tr}(P^{xx}_{k|k,m}); \tag{7.4}$$

and (iii) mean CPU processing time per time step T_{CPU}. When applicable, we replace $\hat{x}_{k|k}$ by either $\hat{x}^{t}_{k|k}$ or $\hat{x}^{p}_{k|k}$ in (7.3) and $P^{xx}_{k|k}$ by either $P^{xxt}_{k|k}$ or $P^{xxp}_{k|k}$ in (7.4).

Fig. 5 shows the state estimates for $x_{2,k}$ and the associated standard deviations for a given simulation of case 1 using UKF, SIUKF, CUKF, CIUKF, IUKF, SUKF, TUKF, TIUKF, PUKF, and PIUKF. According to Fig. 4a, UKF yields the least accurate estimates. A

Table 2

Summary of characteristics of UKF-based algorithms for interval-constrained nonlinear systems. It is shown whether or not the state estimates and the pseudo-error covariance assimilate the interval constraint (4.1) (indicated as □) information in each step of the estimator, namely, the forecast, data assimilation, and truncation/projection steps. NA indicates "nonapplicable" given that the corresponding step does not exist for the algorithm. Also, it is indicated how many constrained optimization problems (COP) are solved at each time step. Moreover, it is indicated which algorithms can handle nonlinear inequality (■), linear equality (☆) and nonlinear equality (★) constraints in addition to interval constraints (□). Specifically, ☆ indicates that if the equality constraint is nonlinear, then the state estimate is not guaranteed to exactly satisfy the constraint, while ★ indicates that if the equality constraint is nonlinear, then the constraint is satisfied at machine precision.

Algorithm	Section	Forecast		Data assimilation		Truncation/projection		COP
		$\hat{x}_{k\|k-1}$	$P^{xx}_{k\|k-1}$	$\hat{x}_{k\|k}$	$P^{xx}_{k\|k}$	$\hat{x}^{p/t}_{k\|k}$	$P^{xxp/t}_{k\|k}$	
UKF [9]	3.2					NA		0
SIUKF [35]	6.1	□	□	☆ ■ □	☆ ■ □	NA		$2n+1$
CUKF	6.2			★ ■ □		NA		1
CIUKF	6.3	□	□	★ ■ □		NA		1
IUKF	6.4	□	□			NA		0
SUKF	6.5			☆ ■ □	☆ ■ □	NA		$2n+1$
PUKF	6.6					★ ■ □		1
PIUKF	6.7	□	□			★ ■ □		1
TUKF	6.8					☆ □	☆ □	0
TIUKF	6.9	□	□			☆ □	☆ □	0

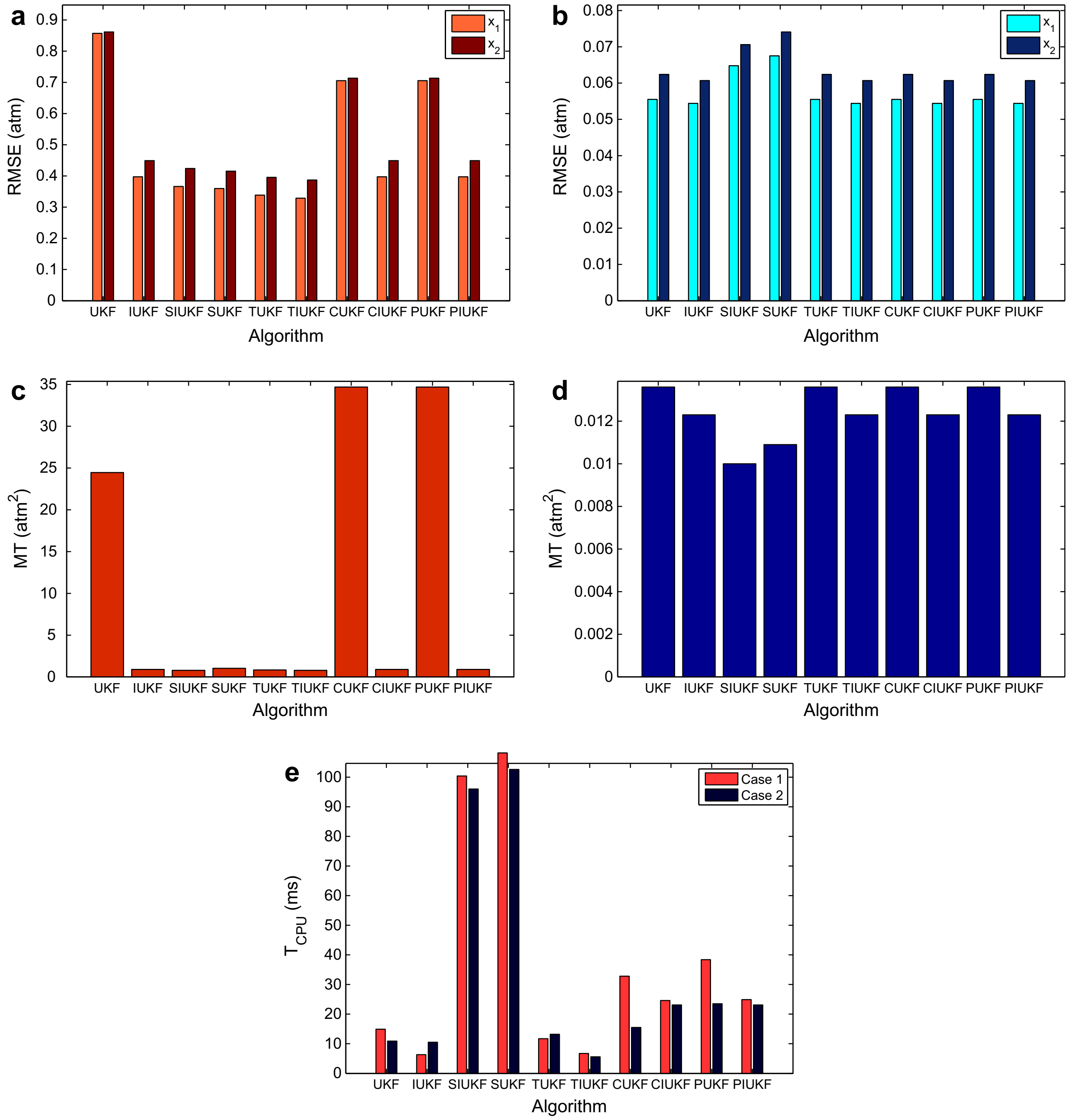

Fig. 4. (a and b) RMSE (7.3), (c and d) MT (7.4), and (e) mean CPU processing time per iteration T_{CPU} for a 100-run Monte Carlo simulation for the batch-reaction system using UKF, IUKF, SIUKF, SUKF, TUKF, TIUKF, CUKF, CIUKF, PUKF, and PIUKF. Case 1 is treated in (a) and (c), while case 2 is treated in (b) and (d).

slight improvement regarding RMSE is achieved by CUKF and PUKF. According to Fig. 5c and Fig. 4c, the poor performance of UKF, CUKF, and PUKF is due to the very slow convergence of the error covariance. Note that TIUKF, TUKF, SIUKF, SUKF, CIUKF, PIUKF, and IUKF produce the best results concerning RMSE and MT.

For case 2, the performance of all algorithms is competitive; see Fig. 4b and d. Actually, SIUKF and SUKF yield slightly less accurate state estimates (larger RMSE) compared to UKF; however, such difference is negligible.

In sum, we observe that methods that assimilate the interval-constraint information in both the state estimate and pseudo-error covariance, namely, CIUKF, SIUKF, SUKF, TUKF, TIUKF, PIUKF, and IUKF, have an improved performance compared to UKF.

When it comes to processing time, as indicated in Fig. 4e, IUKF, TIUKF, and TUKF are quite competitive compared to UKF, which is less than 20% slower than EKF (not shown) for this example. Moreover, CUKF, CIUKF, PIUKF, and PUKF present intermediate processing time, whereas, for this example, SUKF and SIUKF were more than seven times slower than UKF.

7.2. Continuously stirred tank reactor [6,12,33]

We consider the gas-phase, reversible reactions

$$\mathrm{A} \underset{k_2}{\overset{k_1}{\rightleftharpoons}} \mathrm{B} + \mathrm{C},$$

$$2\mathrm{B} \underset{k_4}{\overset{k_3}{\rightleftharpoons}} \mathrm{B} + \mathrm{C},$$

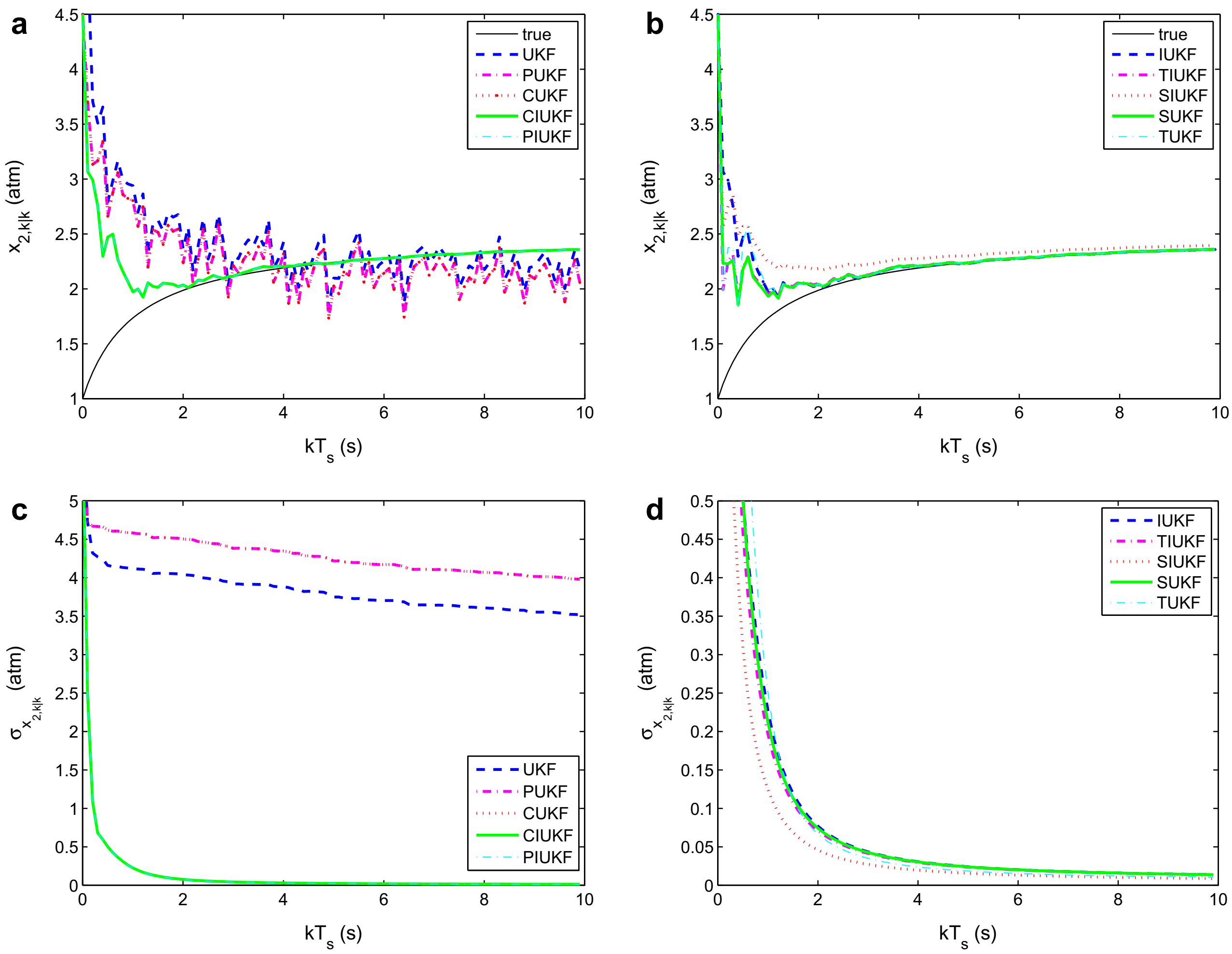

Fig. 5. (a and b) Estimate of $x_{2,k}$ and (c and d) associated standard deviation $\sigma_{x_{2,k}} \triangleq \sqrt{P^{xx}_{(2,2),k|k}}$ for the poor initialization case using (a), (c) UKF, PUKF, CUKF, CIUKF, PIUKF and (b), (d) IUKF, TIUKF, SIUKF, SUKF, TUKF.

with reaction-rate proportions $k_1 = 0.5, k_2 = 0.05, k_3 = 0.2, k_4 = 0.01$, stoichiometric matrix $S = \begin{bmatrix} -1 & 1 & 1 \\ 0 & -2 & 1 \end{bmatrix}$, and reaction rates $r(t) = \begin{bmatrix} k_1 x_1(t) - k_2 x_2(t) x_3(t) \\ k_3 x_2^2(t) - k_4 x_3(t) \end{bmatrix}$. Let the state vector $x(t) \in \mathbb{R}^3_+$ be given by the concentrations of A, B, and C in mol/l. We assume that these reactions take place in a well-mixed, isothermal continuously stirred tank reactor (CSTR), whose dynamics are given by

$$\dot{x}(t) = \frac{1}{3}\left(S^{\mathrm{T}} r(t) + \frac{1}{V_R}([c_f \quad -x(t)]u(t))\right), \tag{7.5}$$

where $V_R = 100$ l is the reactor volume, $c_f = [0.5 \quad 0.05 \quad 0]^{\mathrm{T}}$ mol/l denotes inlet concentrations, $u(t) = [q_f \quad q_o]^{\mathrm{T}}$ is the input vector, and $q_f \geqslant 0$ and $q_o \geqslant 0$ are the volumetric inlet and effluent flow rates. We set $x(0) = [0.5 \quad 0.05 \quad 0]^{\mathrm{T}}$ and $q_f = q_o = 1$.

To perform state estimation using UKF, SIUKF, CUKF, CIUKF, IUKF, SUKF, TUKF, TIUKF, PUKF, and PIUKF, we integrate the process model (7.5) with $T_s = 0.25$ s using the fourth-order Runge–Kutta algorithm such that $x_k \triangleq x(kT_s)$. To help convergence using UKF [38] with $\hat{x}_{0|0} = x_0$, we set $Q_{k-1} = 10^{-6} I_{3\times3}$. For uniformity, this value is used in the remaining cases. Also, we assume the total pressure is measured

$$y_k = [R \quad R \quad R]x_k + v_k, \tag{7.6}$$

where $R = 32.84$ atm×l/mol is a constant, and $R_k = 0.25^2$ is the variance of $v_k \in \mathbb{R}$. We want to enforce the interval constraint (4.1), where $d_k = 0_{3\times1}$ and $e_k = \infty_{3\times1}$. First, we set a poor initialization given by $\hat{x}_{0|0} = [0 \quad 0 \quad 3.5]^{\mathrm{T}}$ and $P^{xx}_{0|0} = 4I_{3\times3}$ and we refer to it as case 1. Case 1 is investigated in [6] using EKF and MHE and in [12] using EKF, UKF, and an algorithm similar to SUKF. We also investigate a second case (case 2) with good initialization given by $\hat{x}_{0|0} = [0.6 \quad 0.1 \quad 0.05]^{\mathrm{T}}$ and $P^{xx}_{0|0} = 0.5I_{3\times3}$.

Fig. 6 presents a performance comparison of the aforementioned algorithms for a 100-run Monte Carlo simulation. Fig. 7 shows the state estimates for $x_{3,k}$ and associated standard deviations for a given simulation. As shown in Fig. 7a, for case 1, UKF does not converge for $kT_s < 180$ s and yields estimates violating (4.1) for $kT_s < 80$ s. Note also that, although CUKF and PUKF slightly improve convergence, they still result in large error; see Fig. 7a and c. On the other hand, SIUKF, SUKF, and the truncation-based algorithms TUKF and TIUKF yield the smallest RMSE indices; see Fig. 6a and b. CIUKF, PIUKF, and IUKF also provide a good performance, although slightly inferior compared to SIUKF, SUKF, TUKF, and TIUKF.

For case 2, unlike the case 2 of the batch reactor example, all constrained algorithms yield more accurate estimates for x_2 and x_3 than UKF; see Fig. 6b and d. However, among the interval-constrained methods, CUKF and PUKF present the worst results. The difference in the performance of SUKF and SIUKF for the good-initialization case (regarding the two examples investigated) is due to the fact that such algorithms (as well as the remaining algorithms investigated in this paper) are approximate for nonlinear systems and, thus, their performance depends on the application.

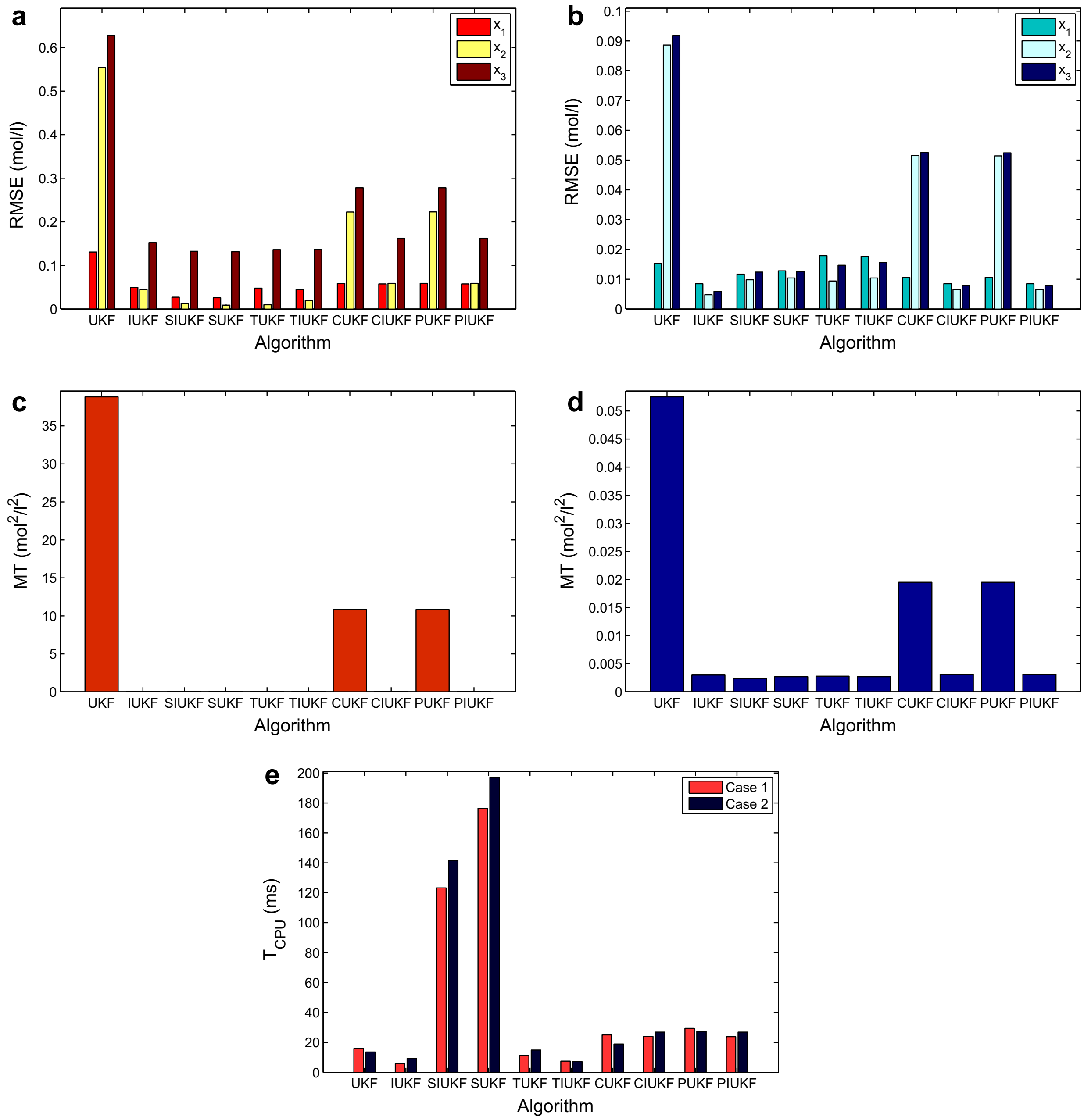

Fig. 6. (a and b) RMSE (7.3), (c and d) MT (7.4), and (e) mean CPU processing time per iteration T_{CPU} for a 100-run Monte Carlo simulation for the CSTR system using UKF, IUKF, SIUKF, SUKF, TUKF, TIUKF, CUKF, CIUKF, PUKF, and PIUKF. Case 1 is treated in (a) and (c), while case 2 is treated in (b) and (d). In (c), the values of MT for IUKF, SIUKF, SUKF, TUKF, TIUKF, CIUKF, and PIUKF are, respectively, given by 0.086, 0.067, 0.068, 0.073, 0.069, 0.085, and 0.085.

In sum, we observe that methods that assimilate the interval-constraint information in both the state estimate and pseudo-error covariance, namely, CIUKF, SIUKF, SUKF, TUKF, TIUKF, PIUKF, and IUKF, have improved performance compared to UKF.

Regarding computational cost, IUKF, TIUKF, and TUKF are competitive with UKF. Also, CUKF, CIUKF, PIUKF, and PUKF are 50% to two times slower than UKF, whose processing time is about 10% larger than the processing time of EKF (not shown) for this example. Furthermore, SIUKF and SUKF are 8–15 times slower than UKF.

For completeness, as done in [6] for this same example, we also include MHE in our performance comparison. We use the MHE implementation of [26]. Table 3 shows the normalized values of RMSE and T_{CPU} for UKF, TIUKF, SIUKF, and MHE, for which we investigate two values of moving horizon size, namely, 2 and 4. We refer to these cases as MHE2 and MHE4, respectively. Except for x_1, RMSE of TIUKF and SIUKF is about five times smaller than the RMSE of UKF. Likewise, the MHE estimates are about five times more accurate than the TIUKF and SIUKF estimates, but at the cost of a substantial increase in the processing time; see Table 3. Note that though MHE yields more accurate estimates than do TIUKF and SIUKF, as suggested in Fig. 7b, the latter algorithms provide good enough estimates. Finally, when the horizon size of MHE is increased from 2 to 4, the improvement in the estimate accuracy does not pay off, having in mind the corresponding increase in the processing time.

8. Concluding remarks

We have addressed the interval-constrained state-estimation problem for nonlinear systems. We have investigated how combi-

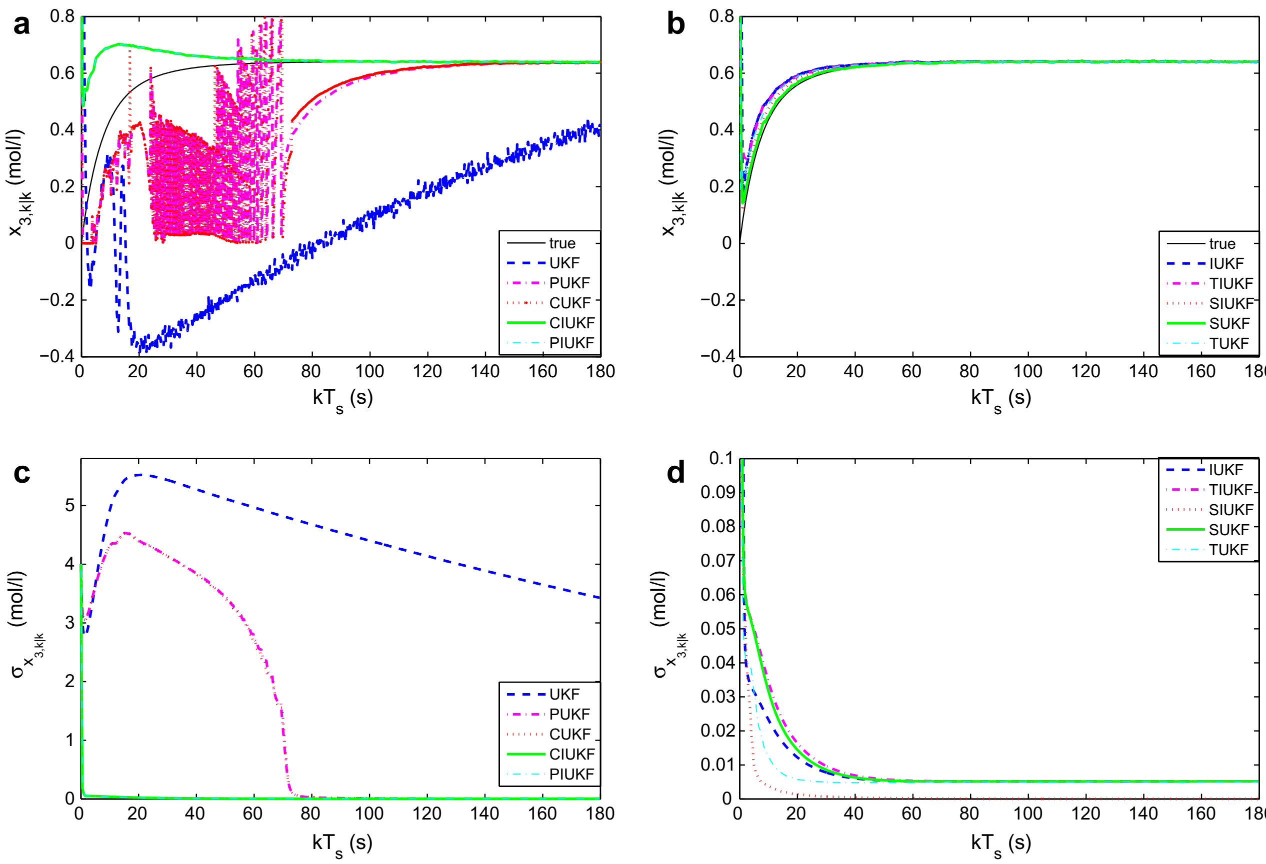

Fig. 7. (a and b) Estimate of $x_{3,k}$ and (c and d) associated standard deviation $\sigma_{x_{3,k}} \triangleq \sqrt{P^{xx}_{(3,3),k|k}}$ for the poor initialization case using (a), (c) UKF, PUKF, CUKF, CIUKF, PIUKF, and (b), (d) IUKF, TIUKF, SIUKF, SUKF, TUKF.

Table 3
RMSE (7.3) and mean CPU processing time per iteration T_{CPU} for a 50-run Monte Carlo simulation for the CSTR system (case 2) using UKF, TIUKF, SIUKF, and MHE. For MHE, two values of moving horizon size are tested, namely, 2 and 4. The indices are normalized by the corresponding values obtained using UKF; see Fig. 6b and e.

	UKF	TIUKF	SIUKF	MHE2	MHE4
$RMSE_1$	1	1.26	0.80	0.393	0.388
$RMSE_2$	1	0.14	0.14	0.033	0.026
$RMSE_3$	1	0.21	0.17	0.040	0.027
T_{CPU}	1	1.17	15.30	200.06	587.60

nations of one out of two candidate unscented approaches for forecast and one out of five candidate methods for data assimilation (see Table 1) can be used. In doing so, we reviewed UKF and SIUKF and introduced CUKF, CIUKF, IUKF, SUKF, TUKF, TIUKF, PUKF, and PIUKF. These methods were compared with relation to whether or not the state estimates, as well as the pseudo-error covariance, are affected by the interval constraint in each step; see Table 2.

We have discussed two illustrative examples, whose state estimates are constrained to be nonnegative. Whenever an interval-constrained algorithm was used, more accurate state estimates were obtained compared to UKF. We observed that, for a good initialization, the performance indices of all constrained algorithms were competitive, occasionally, except for CUKF and PUKF. However, when a poor initialization was set, the UKF estimates violated the interval constraint. In this case, only a slight improvement over UKF was observed using CUKF and PUKF. On the other hand, SIUKF, SUKF, and the truncation-based algorithms TUKF and TIUKF provided the best performance. CIUKF, PIUKF, and IUKF also provided a good performance, although slightly inferior compared to SIUKF, SUKF, TUKF, and TIUKF. In sum, we have observed that methods that enforce the interval-constraint information on both the state estimate and pseudo-error covariance, namely, TUKF, TIUKF, SIUKF, SUKF, IUKF, CIUKF, and PIUKF, provide an improved performance compared to UKF.

Regarding processing time, IUKF, TIUKF, and TUKF were competitive with UKF, since they are not optimization-based algorithms. Therefore, IUKF, TIUKF, and TUKF might be reasonable choices for embedded applications, for instance. Also, CUKF, CIUKF, PIUKF, and PUKF were 50% to three times slower than UKF, whereas SIUKF and SUKF were seven to 15 times slower than UKF. Finally, MHE with horizon size equal to two was around two hundred times slower than UKF. Furthermore, we believe that the processing time of the methods that require the online solving of optimization problems, namely, SIUKF, SUKF, CUKF, CIUKF, PIUKF, and PUKF, are more sensitive to the increase in the dimension of the state vector.

Since the methods investigated in this study are approximate, it is not clear to point out which one is the best method. Instead, it seems that the choice of a method depends on the application. However, from the examples investigated, considering the tradeoff between accuracy and processing time/ease of implementation, TIUKF and TUKF seem to be promising algorithms to enforce interval constraints on nonlinear systems. Compared to MHE, regarding the aforementioned tradeoff, the choice for TIUKF and TUKF may pay off. These truncation-based algorithms enforce the interval constraint on both the state estimate and corresponding error covariance, without the need of solving optimization problems online.

Acknowledgments

Bruno Teixeira, Leonardo Tôrres, and Luis Aguirre are grateful to CNPq and FAPEMIG, Brazil, for financial support. Dennis Bernstein is grateful to the National Science Foundation, under Grants ATM-0417839 and CNS-0539053 to the University of Michigan, USA, for financial support.

Appendix A. The PDF truncation procedure

For completeness, we now review the equations of the PDF-truncation procedure; see [25, pp. 218–222]. The PDF truncation procedure is performed in i steps, where $i = 1, \ldots, n$. Let $\hat{x}^{\mathrm{t}}_{k|k,i}$ and $P^{xx\mathrm{t}}_{k|k,i}$ denote, respectively, the state estimate and the error covariance after enforcing the first $i-1$ rows of the state interval constraint (4.1).

First, at $i = 1$, initialize

$$\hat{x}^{\mathrm{t}}_{k|k,1} = \hat{x}_{k|k} \quad \text{and} \quad P^{xx\mathrm{t}}_{k|k,1} = P^{xx}_{k|k}, \tag{A.1}$$

where $\hat{x}_{k|k}$ and $P^{xx}_{k|k}$ are, respectively, given by (3.15) and (3.16). Then, for $i = 1, \ldots, n$, perform the following four-step loop: (i) find the orthogonal matrix $S \in \mathbb{R}^{n\times n}$ and the diagonal matrix $D \in \mathbb{R}^{n\times n}$ from the Schur decomposition [2, pp. 171–174] of $P^{xx\mathrm{t}}_{k|k,i}$ given by

$$SDS^{\mathrm{T}} = P^{xx\mathrm{t}}_{k|k,i}, \tag{A.2}$$

where $P^{xx\mathrm{t}}_{k|k,i}$ is symmetric by definition; (ii) perform Gram-Schmidt orthogonalization to find the orthogonal matrix $\Theta \in \mathbb{R}^{n\times n}$ satisfying

$$\Theta D^{1/2}\mathrm{col}_i(S^{\mathrm{T}}) = \left[\sqrt{P^{xx\mathrm{t}}_{(i,i),k|k,i}} \quad 0_{1\times(n-1)} \right]^{\mathrm{T}},$$

which is given by

$$\mathrm{row}_l(\Theta) = \begin{cases} \dfrac{1}{\sqrt{P^{xx\mathrm{t}}_{(i,i),k|k,i}}}\mathrm{row}_i(S)D^{1/2}, & l = 1, \\ \left(e_l - \sum\limits_{q=1}^{l-1}\left(e_l^{\mathrm{T}}\mathrm{col}_q(\Theta^{\mathrm{T}})\right)\mathrm{col}_q(\Theta^{\mathrm{T}})\right)^{\mathrm{T}}, & l = 2, \ldots, n, \end{cases} \tag{A.3}$$

where $e_l \triangleq \mathrm{col}_l(I_{n\times n})$, if $\mathrm{row}_l(\Theta) = 0_{1\times n}$, then reset

$$\mathrm{row}_l(\Theta) = \left(e_1 - \sum_{q=1}^{l-1}\left(e_1^{\mathrm{T}}\mathrm{col}_q(\Theta^{\mathrm{T}})\right)\mathrm{col}_q(\Theta^{\mathrm{T}})\right)^{\mathrm{T}}; \tag{A.4}$$

also, normalize

$$\mathrm{row}_l(\Theta) = \frac{1}{||\mathrm{row}_l(\Theta)||_2}\mathrm{row}_l(\Theta), \quad l = 1, \ldots, n; \tag{A.5}$$

(iii) find the parameters of the interval constraint $a_{k,i} \leqslant z_{i,k,i} \leqslant b_{k,i}$, where $a_{k,i} < b_{k,i} \in \mathbb{R}$ are given by

$$a_{k,i} = \frac{1}{\sqrt{P^{xx\mathrm{t}}_{(i,i),k|k,i}}}(d_{i,k} - x^{\mathrm{t}}_{i,k|k,i}), \tag{A.6}$$

$$b_{k,i} = \frac{1}{\sqrt{P^{xx\mathrm{t}}_{(i,i),k|k,i}}}(e_{i,k} - x^{\mathrm{t}}_{i,k|k,i}) \tag{A.7}$$

and $z_{k,i} \triangleq \Theta D^{-1/2}S^{\mathrm{T}}(x_k - \hat{x}^{\mathrm{t}}_{k|k,i}) \in \mathbb{R}^n$ with mean

$$\hat{z}_{k,i} = \left[\mu_i \quad 0_{1\times(n-1)}\right]^{\mathrm{T}} \tag{A.8}$$

and covariance

$$P^{zz}_{k,i} = \mathrm{diag}\left(\sigma_i^2, 1_{1\times(n-1)}\right), \tag{A.9}$$

where

$$\alpha_i = \frac{\sqrt{2}}{\sqrt{\pi}\left[\mathrm{erf}\left(\frac{b_{k,i}}{\sqrt{2}}\right) - \mathrm{erf}\left(\frac{a_{k,i}}{\sqrt{2}}\right)\right]}, \tag{A.10}$$

$$\mu_i = \alpha_i\left[\exp\left(\frac{-a^2_{k,i}}{2}\right) - \exp\left(\frac{-b^2_{k,i}}{2}\right)\right], \tag{A.11}$$

$$\sigma_i^2 = \alpha_i\left[\exp\left(\frac{-a^2_{k,i}}{2}\right)(a_{k,i} - 2\mu_i) - \exp\left(\frac{-b^2_{k,i}}{2}\right)(b_{k,i} - 2\mu_i)\right] + \mu_i^2 + 1, \tag{A.12}$$

where

$$\mathrm{erf}(t) \triangleq \frac{2}{\sqrt{\pi}}\int_0^t \exp(-\tau^2)d\tau$$

is the error function; and (iv) perform the inverse transformation

$$\hat{x}^{\mathrm{t}}_{k|k,i+1} = SD^{1/2}\Theta^{\mathrm{T}}\hat{z}_{k,i} + \hat{x}^{\mathrm{t}}_{k|k,i}, \tag{A.13}$$

$$P^{xx\mathrm{t}}_{k|k,i+1} = SD^{1/2}\Theta^{\mathrm{T}}P^{zz}_{k,i}\Theta D^{1/2}S^{\mathrm{T}}. \tag{A.14}$$

Finally, at $i = n$, we set

$$\hat{x}^{\mathrm{t}}_{k|k} = \hat{x}^{\mathrm{t}}_{k|k,n+1}, \tag{A.15}$$

$$P^{xx\mathrm{t}}_{k|k} = P^{xx\mathrm{t}}_{k|k,n+1}. \tag{A.16}$$

References

[1] M.S. Arulampalam, S. Maskell, N. Gordon, T. Clapp, A tutorial on particle filters for online nonlinear/non-Gaussian Bayesian tracking, IEEE Transactions on Signal Processing 50 (2) (2002) 174188.
[2] D.S. Bernstein, Matrix Mathematics, Princeton University Press, Princeton, USA, 2005.
[3] M. Chaves, E.D. Sontag, State-estimators for chemical reaction networks of Feinberg–Horn–Jackson zero deficiency type, European Journal of Control 8 (2002) 343–359.
[4] S. Gillijns, O.B. Mendoza, J. Chandrasekar, B.L.R. De Moor, D.S. Bernstein, A. Ridley, What is the ensemble Kalman filter and how well does it work? in: Proceedings of the 2006 American Control Conference, Minneapolis, USA, 2006, pp. 4448–4453.
[5] G.C. Goodwin, M.M. Seron, J.A. de Doná, Constrained Control and Estimation: An Optimisation Approach, Springer, 2005.
[6] E.L. Haseltine, J.B. Rawlings, Critical evaluation of extended Kalman filtering and moving-horizon estimation, Industrial and Engineering Chemistry Research 44 (8) (2005) 2451–2460.
[7] A.H. Jazwinski, Stochastic Processes and Filtering Theory, Academic Press Inc., New York City, 2007. reprinted by Dover, 2007.
[8] S.J. Julier, J.J. LaViola Jr., On Kalman filtering with nonlinear equality constraints, IEEE Transactions on Signal Processing 55 (6) (2007) 2774–2784. June.
[9] S.J. Julier, J.K. Uhlmann, Unscented filtering and nonlinear estimation, Proceedings of the IEEE 92 (2004) 401–422.
[10] S.J. Julier, J.K. Uhlmann, Hugh F. Durrant-Whyte, A new method for the nonlinear transformation of means and covariances in filters and estimators, IEEE Transactions on Automatic Control 45 (3) (2000) 477–482.
[11] R. Kandepu, B.A. Foss, L. Imsland, Applying the unscented Kalman filter for nonlinear state estimation, Journal of Process Control 18 (7-8) (2008) 753–768.
[12] S. Kolas, B.A. Foss, T.S. Schei, Constrained nonlinear state estimation based on the UKF approach, Computers and Chemical Engineering 33 (8) (2009) 1386–1401.
[13] L. Lang, W. Chen, B.R. Bakshi, P.K. Goel, S. Ungarala, Bayesian estimation via sequential Monte Carlo sampling – constrained dynamic systems, Automatica 43 (2007) 1615–1622.
[14] T. Lefebvre, H. Bruyninckx, J. De Schutter, Kalman filters for nonlinear systems: a comparison of performance, International Journal of Control 77 (7) (2004) 639–653.
[15] D. Massicotte, R.Z. Morawski, A. Barwicz, Incorporation of a positivity constraint into a Kalman-filter-based algorithm for correction of spectrometric data, IEEE Transactions on Instrumentation and Measurement 44 (1) (1995) 2–7.
[16] S. Narasimhan, R. Rengaswamy, Reply to 'Comments on "Robust and reliable estimation via unscented recursive nonlinear dynamic data reconciliation"', Journal of Process Control 19 (4) (2009) 719–721.
[17] J. Prakash, S.C. Patwardhan, S.L. Shah, Constrained State estimation using the ensemble Kalman filter, in: Proceedings of the 2008 American Control Conference, Seattle, USA, 2008, pp. 3542–3547.
[18] C.V. Rao, J.B. Rawlings, J.H. Lee, Constrained linear state estimation – a moving horizon approach, Automatica 37 (10) (2001) 1619–1628.

[19] C.V. Rao, J.B. Rawlings, D.Q. Mayne, Constrained state estimation for nonlinear discrete-time systems: stability and moving horizon approximations, IEEE Transactions on Automatic Control 48 (2) (2003) 246–258.
[20] J.B. Rawlings, B.R. Bakshi, Particle filtering and moving horizon estimation, Computers and Chemical Engineering 30 (10–12) (2006) 1529–1541.
[21] D.G. Robertson, J.H. Lee, On the use of constraints in least squares estimation and control, Automatica 38 (2002) 1113–1123.
[22] M. Rotea, C. Lana, State estimation with probability constraints, International Journal of Control 81 (6) (2008) 920–930.
[23] L.P. Russo, R.E. Young, Moving horizon state estimation applied to an industrial polymerization process, in: Proceedings of the 1999 American Controle Conference, vol. 2, San Diego, USA, 1999, pp. 1129–1133.
[24] N. Shimada, Y. Shirai, Y. Kuno, J. Miura, Hand gesture estimation and model refinement using monocular camera – Ambiguity limitation by inequality constraints, in: Proceedings of the Third IEEE International Conference on Automatic Face and Gesture Recognition, Nara, Japan, 1998, pp. 268–273.
[25] D. Simon, Optimal State Estimation: Kalman, H_∞ and Nonlinear Approaches, Wiley-Interscience, 2006.
[26] D. Simon, Kalman filtering with state constraints: a survey of linear and nonlinear algorithms, IET Control Theory and Applications (in press). Available: http://academic.csuohio.edu/simond/ConstrKF/ConstrKF.pdf, 2009.
[27] D. Simon, T. Chia, Kalman filtering with state equality constraints, IEEE Transactions on Aerospace and Electronic Systems 38 (1) (2002) 128–136.
[28] D. Simon, D.L. Simon, Kalman filtering with inequality constraints for turbofan engine health estimation, IEE Proceedings – Control Theory and Applications 153 (3) (2006) 371–378.
[29] B.O.S. Teixeira, Constrained state estimation for linear and nonlinear dynamic systems, Ph.D. Thesis, Graduate Program in Electrical Engineering, Federal University of Minas Gerais, Belo Horizonte, Brazil, 2008.
[30] B.O.S. Teixeira, J. Chandrasekar, H.J. Palanthandalam-Madapusi, L.A.B. Tôrres, L.A. Aguirre, D.S. Bernstein, Gain-constrained Kalman filtering for linear and nonlinear systems, IEEE Transactions on Signal Processing 56 (9) (2008) 4113–4123.
[31] B.O.S. Teixeira, J. Chandrasekar, L.A.B. Tôrres, L.A. Aguirre, D.S. Bernstein, State estimation for linear and nonlinear equality-constrained systems, International Journal of Control 82 (5) (2009) 918–936.
[32] B.O.S. Teixeira, M.A. Santillo, R.S. Erwin, D.S. Bernstein, Spacecraft tracking using sampled-data Kalman filters, IEEE Control Systems Magazine 28 (4) (2008) 78–94.
[33] B.O.S. Teixeira, L.A.B. Tôrres, L.A. Aguirre, D.S. Bernstein, Unscented filtering for interval-constrained nonlinear systems, in: Proceedings of the 47th IEEE Conference on Decision and Control, Cancun, Mexico, 2008, pp. 5116–5121.
[34] S. Ungarala, E. Dolence, K. Li. Constrained extended Kalman filter for nonlinear state estimation, in: Proceedings of the Eighth International IFAC Symposium on Dynamics and Control of Process Systems, vol. 2, Cancun, Mexico, 2007, pp. 63–68.
[35] P. Vachhani, S. Narasimhan, R. Rengaswamy, Robust and reliable estimation via unscented recursive nonlinear dynamic data reconciliation, Journal of Process Control 16 (10) (2006) 1075–1086.
[36] P. Vachhani, R. Rengaswamy, V. Gangwal, S. Narasimhan, Recursive estimation in constrained nonlinear dynamical systems, AIChE Journal 51 (3) (2005) 946–959.
[37] R. van der Merwe, E.A. Wan, S.J. Julier, Sigma-point Kalman filters for nonlinear estimation and sensor-fusion – applications to integrated navigation, in: Proceedings of the AIAA Guidance, Navigation and Control Conference, Providence, USA, n. 2004-5120, 2004.
[38] K. Xiong, H. Zhang, C. Chan, Author's reply to Comments on 'Performance evaluation of UKF-based nonlinear filtering', Automatica 43 (2007) 569–570.
[39] V.M. Zavala, C.D. Laird, L.T. Biegler, A fast moving horizon estimation algorithm based on nonlinear programming sensitivity, Journal of Process Control 18 (9) (2008) 876–884.